Materials Transactions, Vol. 44, No. 12 (2003) pp. 2688 to 2694

Mechanical Properties of Friction Surfaced 5052 Aluminum Alloy*1

Hidekazu Sakihama*2, Hiroshi Tokisue and Kazuyoshi Katoh

College of Industrial Technology, Nihon University, Narashino 275-8575, Japan

5052 aluminum alloy used for substrate and consumable rod, was friction surfaced using a numerical controlled full automatic friction welding machine. Effects of the surfacing conditions on some characteristics of deposits were investigated. It was clearly observed that the circularly pattern appeared on the surface of deposit by the rotation of consumable rod. The deposit has a tendency to incline toward the advancing side further than center of deposit for the feed direction of consumable rod. This deviation accompanied the decrease of the rotational speed of consumable rod. The width of deposit increased with increasing friction pressure, and decreasing rotational speed of consumable rod. The thickness of deposit became thinner when the consumable rod was high revolution. The surfacing efficiency decreased with increasing friction pressure and rotational speed of consumable rod, but increased with increasing feed speed. Microstructure of the deposit was finer than that of the substrate and consumable rod. The softened area was recognized at 3 mm distance from the weld interface of substrate. The tensile strength of deposit increased with increasing friction pressure. The maximum tensile strength of deposits showed 88.8% of the base metal of substrate.

(Received June 18, 2003; Accepted October 7, 2003)

Keywords: *friction surfacing, 5052 aluminum alloy, mechanical properties, microstructure, deposit, consumable rod*

1. Introduction

From old times, various methods such as plating, deposition and spraying have been attempted and commercialized to surface modify materials. Each of these methods, however, involves complex procedures and requires numerous processes. The friction surfacing is a potential surface modification method, the principle of which is relatively simple, with which coating would be enabled after rebuilt of friction welding machines. This method is superior with respect to resource and energy conservation. However, there are very few reports of friction surface modification,[1,2] and very few instances of its practical application have been reported. Also, most coating methods used for repairing castings consist of arc or gas welding[3]; therefore, the type of materials used limits applicable coating materials. On the other hand, based on the fact that friction surfacing, whose procedure is similar to the principle of friction welding, is a form of solid state bonding, a wide variety of combinations of materials are possible, and additional function might be given to surfacing. Surfacing can be done at low temperatures because surface modification takes place in the solid phase; therefore, minimal thermal effects on the materials can be anticipated.

This paper deals with characteristics of friction surfaced material, combining 5052 aluminum alloy plate and bar used for the purpose of obtaining basic data on the friction surfaces.

2. Materials and Experimental Procedure

5052 P-H34 aluminum alloy plate of 5 mm thickness as a substrate was machined by cutting down to 50 mm width 150 mm length. And, as a consumable rod, 5052 BDS-F aluminum alloy bar of 20 mm in diameter was used machining it down to 100 mm length. The chemical compositions and mechanical properties of two base metals are shown in Tables 1 and Table 2, respectively.

Table 1 Chemical compositions of materials (mass%).

Material	Si	Fe	Cu	Mn	Mg	Cr	Zn	Al
Rod	0.13	0.15	0.03	0.04	2.24	0.15	0.02	bal.
Plate	0.09	0.27	0.02	0.03	2.49	0.18	-	bal.

Table 2 Mechanical properties of materials.

Material	Tensile strength (MPa)	Elongation (%)	Hardness (HV0.1)
Rod	245	16.2	81.0
Plate	256	13.4	72.3

Table 3 Friction surfacing conditions.

Friction pressure, P (MPa)	20, 25, 30, 35, 40
Rotational speed, N (s^{-1})	16.7, 25.0, 33.3, 41.7, 50.0
Traverse speed, f ($mm \cdot s^{-1}$)	5, 7, 9, 11

Friction surfacing was performed under the surfacing conditions shown in Table 3, using a surfacing device equipped on the pressure device of numerically controlled full automatic friction welding machine. The friction surfacing was performed by maintaining contact between substrate and consumable rod for 1 second and then moving substrate, and was continued until consumable rod was worn down by 30 mm.

Observation of the outside appearance and structure, hardness measurement and tensile tests of the deposit and substrate were conducted at room temperature. The shape of tensile test specimen is shown in Fig. 1, and deposit and

*1This Paper was Originally Published in the Japan Institute of Light Metals, **52**-8 (2002), 346-351.

*2Graduate Student, Nihon University. Present address: Showa Denko K.K., Oyama 323-8678, Japan.

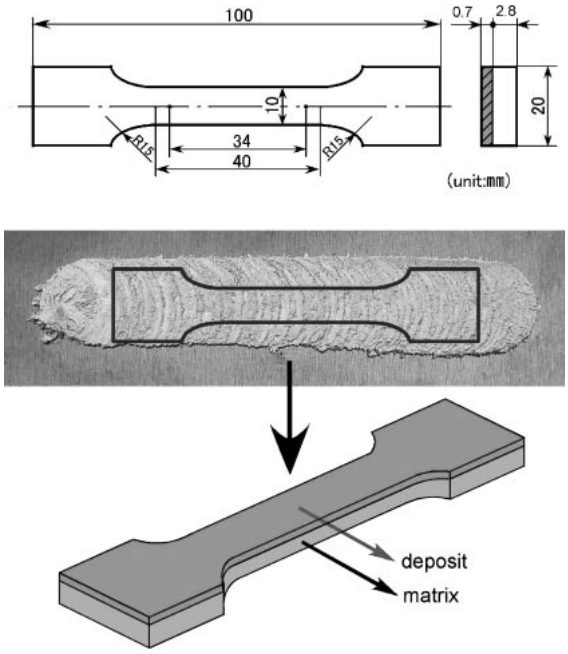

Fig. 1 Sampling position and size of tensile test specimen.

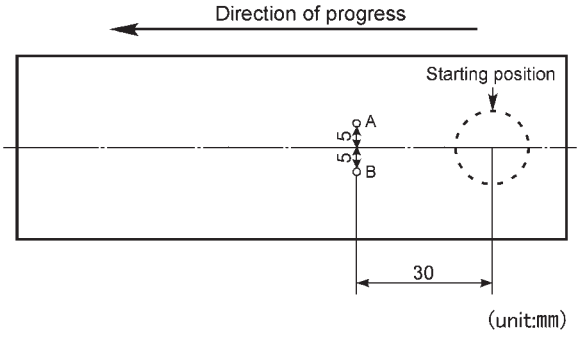

Fig. 2 Measurement positions of temperature.

substrate, which were machined into thickness of 0.7 mm and 2.8 mm, respectively, were tested. Holes for the thermocouples were prepared as shown in Fig. 2, the thermocouples were inserted from the back of substrate so as to make contact between its tip and the surface of substrate, to determine the temperature during friction surfacing process.

3. Experimental Results and Discussion

3.1 Observation of deposit

The quantity of deposit depended on the coating conditions, since surfacing was controlled according to the length of consumable rod. Accordingly, appearance of the deposit differs according to the coating conditions. The appearance after surfacing is shown in Fig. 3. It was clearly observed that the circularly patterns appeared on the substrate by the rotation of consumable rod, regardless of the rotational speed of consumable rod. The appearance of deposit was similar to low alloy steel surfaced with mild steel.[2] The intervals between these circularly pattern, as well as the width of deposit, tended to become narrower with more rapid rotation of consumable rod. The deposit has a tendency to

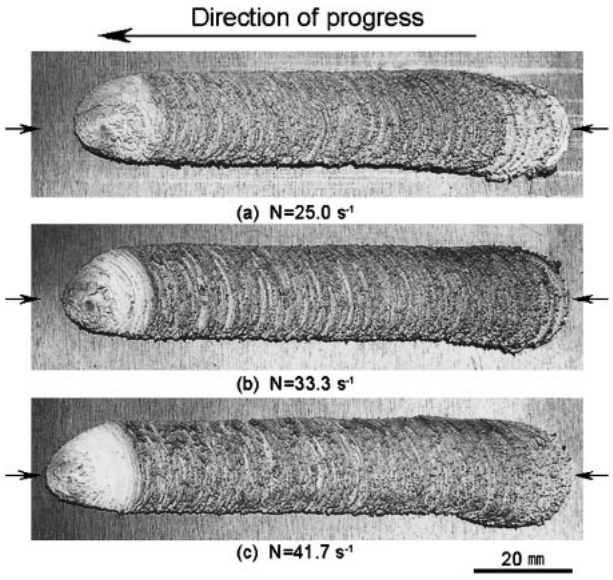

Fig. 3 Appearances of deposit under conditions of friction pressure 30 MPa and traverse speed 9 mm·s^{-1}. The arrows show center of consumable rod.

incline toward to the advancing side further than center of the deposit for the feed direction of consumable rod, which became greater with decreasing rotational speed of consumable rod. The degree of deviation from the center of rotation on the consumable rod showed as 3.52, 2.31 and 1.78 mm at rotational speeds of 25.0, 33.3 and 41.7 s^{-1}, respectively, under the surfacing conditions shown in Fig. 3.

This may be due to the dynamic relationship between direction of rotation and movement of consumable rod. A force will be generated in the direction in which the direction of rotation and shift of consumable rod conform, *i.e.*, on the advancing side of the surfaced area in this experiment, in the direction, which the consumable rod is shifted forward. On the retreating side, the force will be generated in the direction in which the consumable rod is shifted backward. This might be because the consumable rod was clustered on the advancing side along which it is shifted. It has been reported that the same effect can be observed on friction surfaced mild steel.[2]

The effects of the rotational speed of consumable rod on the thickness, width, and extension of the deposit are shown in Fig. 4. The deposit tended to be greater in thickness with increasing rotational speed of consumable rod, regardless of the traverse speed and friction pressure. As shown in the report on friction welding,[4] this might be due to an increase in torque during friction with decreased rotational speed and due to an increase in the thickness of deposit because of an increased rate of deformation of consumable rod. The effect of traverse speed and friction pressure on the thickness of deposit was decreased with increasing rotational speed of consumable rod, making the thickness of deposit almost uniform at rotational speed of 50.0 s^{-1}.

The width of the deposit tended to decrease with increased rotational speed and traverse speed of consumable rod, but it was almost uniform under the conditions of the rotation of consumable rod was slow, because effect of the traverse speed was limited. This might be because width of the

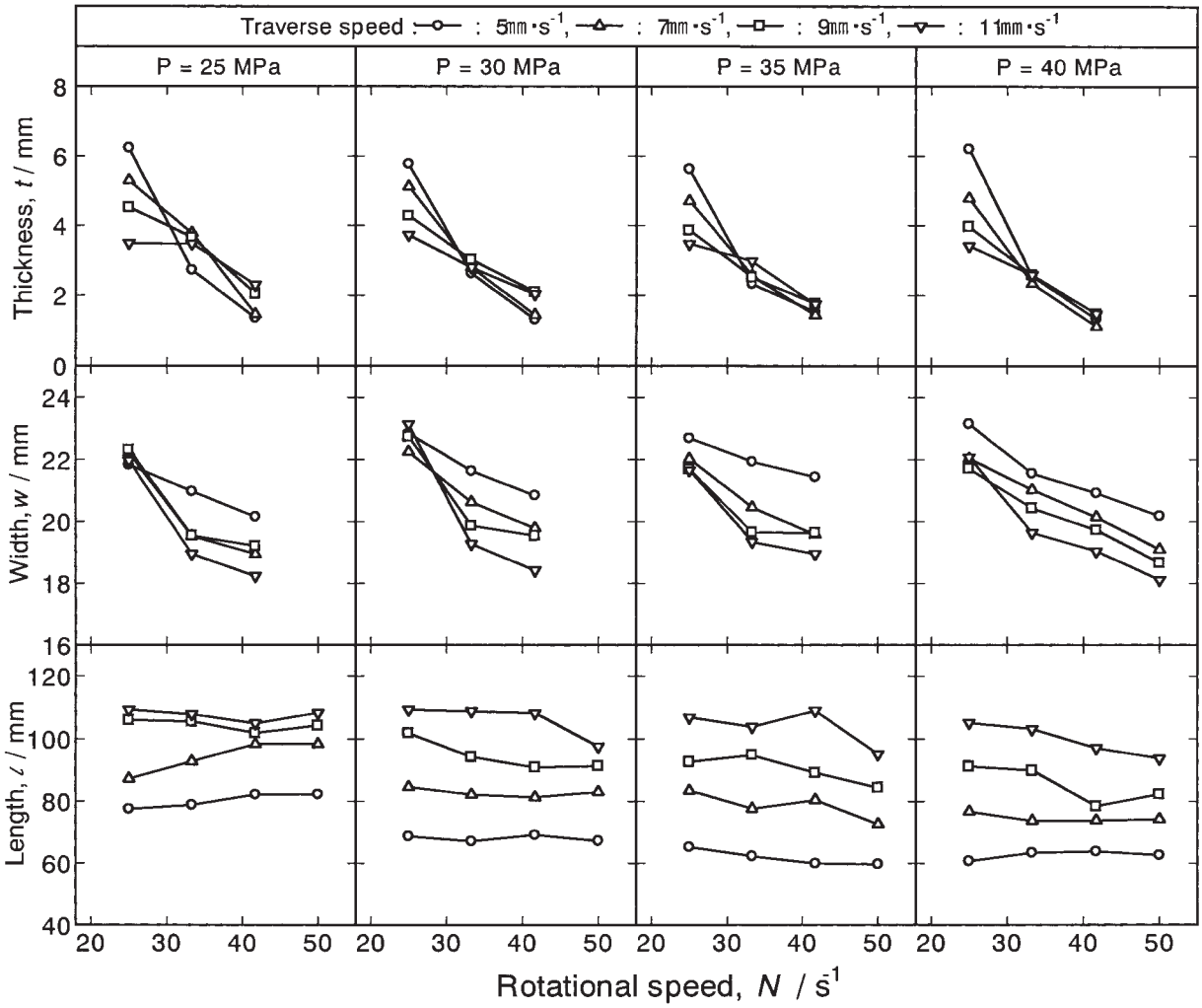

Fig. 4 Relation between rotational speed and thickness, width and length of deposit.

deposit may be decreased by a decrease in the closure area of substrate and consumable rod, for the identical reason for the decrease in the closure area seen during friction with increasing rotational speed of consumable rod which is exhibited during friction welding.[5)]

Concerning the traveling phenomena of the rotational plane observed the friction welding process, which would be similar to that observed the friction surfacing process, it was reported in an experiment using SS400 and SUS403 steels that the traveling distance in the rotational plane, which is friction welding (corresponding to the thickness of deposit in this experiment), would be decreased when the rotation of the principal axis was increased.[4)]

Concerning the extension of deposit, the ideal maximum extension of deposit is 110 mm; that is, sum of the traveling distance of consumable rod, which is mechanically limited to 90 mm along substrate, and 20 mm diameter of consumable rod. The effect of the rotational speed of consumable rod on the extension of deposit was small, compared with the changes in its thickness and width. The extension reached almost 110 mm at a traverse speed of 9 mm·s^{-1} or more under the condition of a low friction pressure of 25 MPa regardless of the rotational speed of consumable rod. The extension of the deposit tended to be decreased slightly with increased rotational speed of consumable rod under the conditions of high friction pressure and high traverse speed.

Not all the consumable rod consumed can be deposited on the substrate during friction surfacing; a proportion of consumable rod is discharged outside as burrs similar to those generated the friction welding. The macrostructure of consumable rod after surfacing is shown in Fig. 5. Regardless of the surfacing conditions, residual burrs on the consumable rod had a similar appearance to those on the friction welded joints.[6)]

Based on the assumption that determination of surfacing efficiency (ratio of weight of the consumable rod before and after surfacing) associated with width and thickness of the deposit could provide insight into the relationship between them, we attempted to determine surfacing efficiency. The results of measurement of surfacing efficiency are shown in Fig. 6. It chose that was a setting of 30 mm of the consumed length of consumable rod. There were almost no variations in the length actually consumed under identical conditions. However, variations were observed under different coating conditions. In this experiment, the maximum difference among consumed lengths of consumable rod was a very small 0.66 mm, which would cause no practical problems.

Surfacing efficiency was reduced by an increase in friction

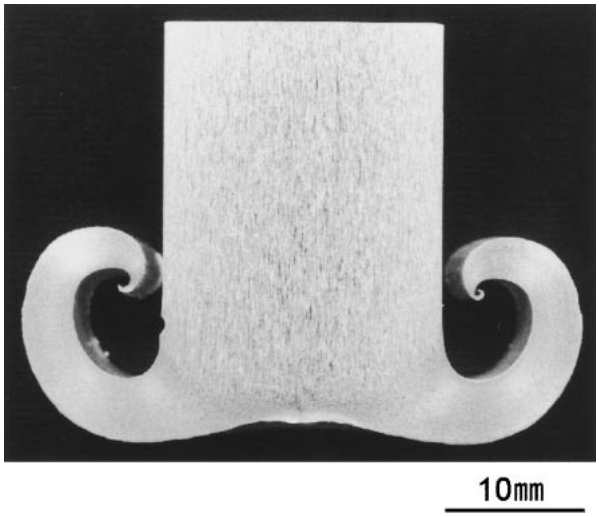

Fig. 5 Macrostructure of consumable rod after friction surfacing under condition of friction pressure 30 MPa, rotational speed 41.7 s^{-1} and traverse speed 9 mm·s^{-1}.

pressure and rotational speed of consumable rod; rotational speed in particular had a significant influence. Also, it tended to improve with increasing the traverse speed of substrate. The low surfacing efficiency might have been due to increased discharge of consumable rod as burrs, which in turn may be caused by the increased skidding between consumable rod and friction surface seen by increasing the rotational speed of consumable rod.

3.2 Observation of structure

Cross sectional microstructures of the deposit is shown in Fig. 7. The weld interface can be clearly distinguished between deposit and substrate of the surfaced specimen (Fig. 7(a)) at 20 MPa, the lowest friction pressure applied in this experiment, and a small amount of incomplete weld was observed at both sides of the deposit. This might be because the friction pressure might not be transmitted effectively to the outer regions of consumable rod if the pressure is decreased due to burrs produced from the consumable rod. A small amount of defective weld was observed on the weld interface. This defective weld disappeared at high friction pressures: no defective welding at all was observed at a pressure of 40 MPa (Fig. 7(b)). The weld interface proved more difficult to categorize into the deposit and substrate at higher friction pressure, and there were not welded parts observed on either side of deposit, indicating that the entire surface of deposit was welded completely.

Microstructures of near the weld interface is shown in Fig. 8. Microstructure of the deposit was finer than that of the consumable rod and substrate. The substrate near the weld interface has a fine structure, which appeared to be processed, and in the peripheral area, due to heating, there was a slightly coarser structure than that of the substrate. A similar structure was observed under other conditions; there was no significant difference in structure attributable to the surfacing conditions.

3.3 Temperature-time history of the friction surfacing process

Figure 9 shows a temperature-time history during the friction surfacing process at the measurement points shown in Fig. 2. During friction surfacing, the temperature started to increase immediately after initiation of friction, and the

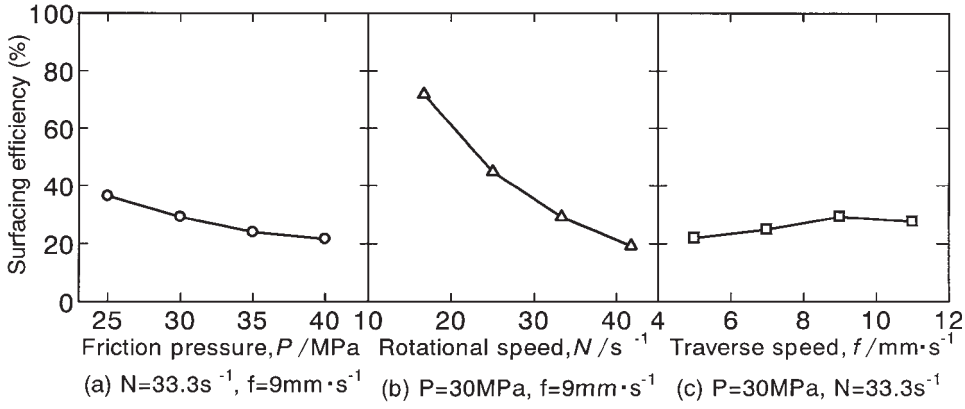

Fig. 6 Effect of friction surfacing conditions on surfacing efficiency.

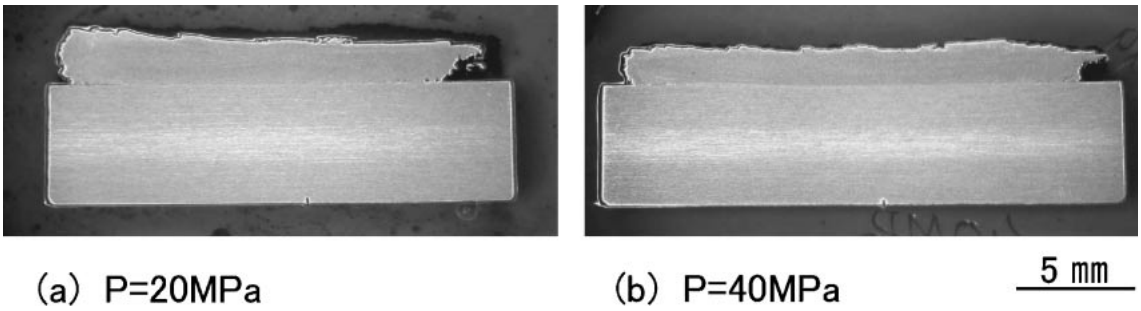

Fig. 7 Macrostructures of deposit under conditions of rotational speed 41.7 s^{-1} and traverse speed 9 mm·s^{-1}.

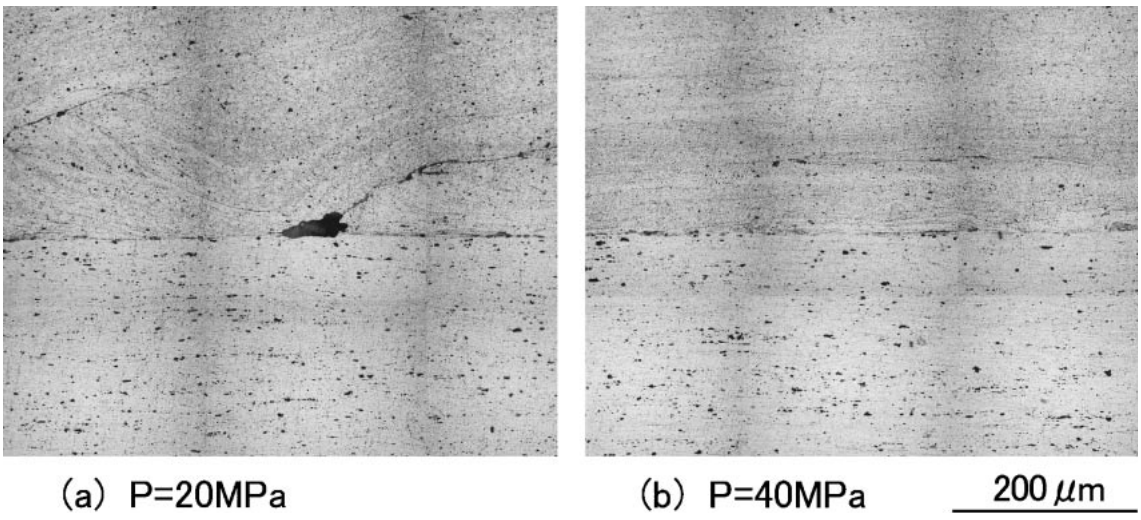

Fig. 8 Microstructures of deposit under conditions of rotational speed 41.7 s^{-1} and traverse speed 9 mm·s^{-1}.

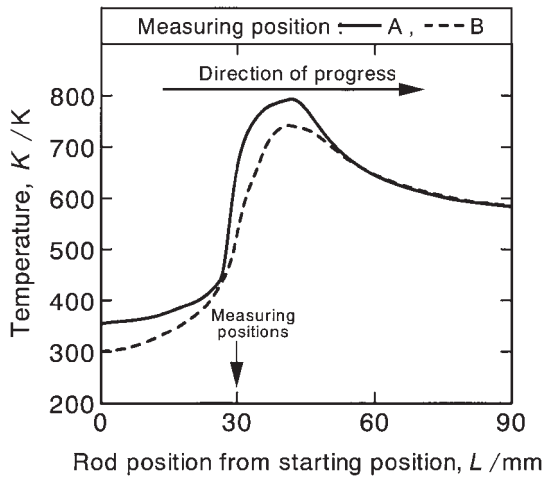

Fig. 9 Temperature-time histories of friction surfacing process under conditions of friction pressure 30 MPa, rotational speed 41.7 s^{-1} and traverse speed 9 mm·s^{-1}.

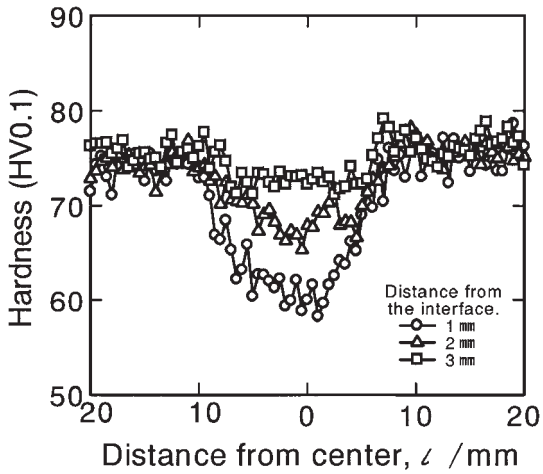

Fig. 10 Hardness distributions of deposit under conditions of friction pressure 30 MPa, rotational speed 41.7 s^{-1} and traverse speed 9 mm·s^{-1}.

gradient became steeper when the consumable rod as a heat source came closer to the measurement point. The temperature increased slightly when the consumable rod reached and left it, and then decreased in the material at increasing distance from the measurement point. The upper limit of the temperature range was lower by about 100-150 K than that of the friction welding,[7,8] suggesting that the substrate temperature did not match that seen the friction welding. The reason for this is that relative linear motion occurs between the consumable rod and substrate in friction surfacing, whereas in friction welding, the friction area always represents a weld interface without any shift in friction area, despite the fact that burn-off length was produced during the friction process.

The temperature on the advancing side was higher value such as about 52 K than that of the retreating side, indicating good agreement with the fact that deposits were clustered on the advancing side in which consumable rod was shifted, as described in appearance observation above. There was almost no difference in temperature-time history and the upper limit of temperature range among the measurement points.

3.4 Hardness distribution

Figure 10 shows the hardness distribution within the substrate immediately below the deposit. There was a softening area at 1 mm, the nearest point from the deposit, and the hardness of softest point was similar to that of the substrate with O-treatment. The width of softening area showed good correspondence with that of the deposit. With increasing distance from the deposit, the softening area became narrower and the hardness of softest point was increased; there was almost no softening area at 3 mm from the weld interface of substrate. The width of softening area associated with the heat of friction welded aluminum alloy joint was 15-20 mm from the weld interface.[7,8] The width of heat affected zone was narrower on the friction surface. This might be due to the lower temperatures seen during surfacing than during friction welding. The mean hardness within the deposit was determined to be 57 HV, which was similar to that of aluminum alloy with O-treatment.

3.5 Tensile test

Results of the tensile tests are shown in Fig. 11. Tensile strength showed a slight increase with increased rotational

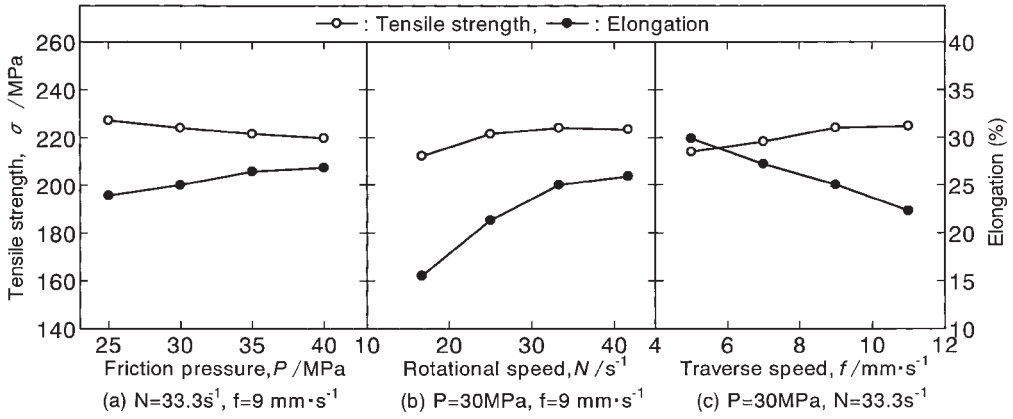

Fig. 11 Results of tensile test of deposits.

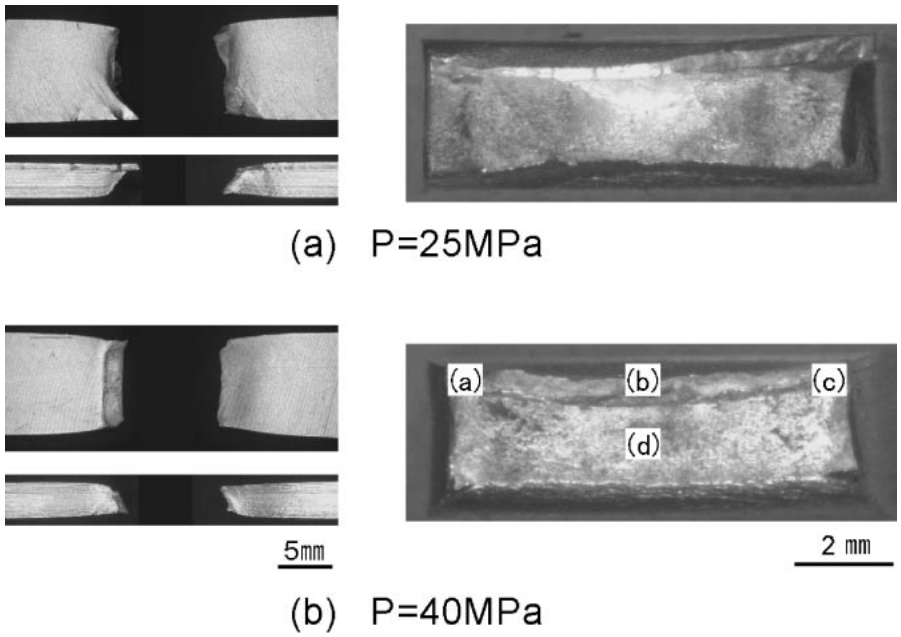

Fig. 12 Appearances and macrofractographs of tensile tested specimens under conditions of rotational speed 33.3 s^{-1} and traverse speed 9 $mm \cdot s^{-1}$.

speed and traverse speed of consumable rod, and tended to decrease slightly with increasing friction pressure. In this experiment, the highest tensile strength was obtained at a friction pressure of 25 MPa, rotational speed of 33.3 s^{-1}, and traverse speed of 9 $mm \cdot s^{-1}$, and showed 88.8% of the base metal of substrate. The elongation under any conditions was higher than that of the base metal of substrate, whose value increased with an increase in the friction pressure and rotational speed of consumable rod, and decreased with increasing the traverse speed as distinct from the tensile strength. As described above, these findings may be explained by the effect of difference between the hardness and width of the softening area within the substrate, associated with the thermal effect, due to differences in the upper limit of the temperature range during surfacing.

Figure 12 shows the appearance and macrofractographs of the tensile fractured surfaces. The upper side is the surface of deposit. At a low friction pressure of 25 MPa (Fig. 12(a)), poor conjugation between deposit and substrate was observed due to a lower upper limit of the temperature range compared with that under other conditions, and flaking was observed between both. In the tested specimen with high tensile strength (Fig. 12(b)), both deposit and substrate extended, and there was no flaking between either.

Figure 13 shows macrofractographs (a) to (d) in Fig. 12(b). It showed ductile fractured surfaces in which dimples are observed everywhere. However, dimples within the deposit were slightly finer than those of the substrate. On the advancing side of deposit was clustered, there are many more fine dimples (Fig. 13(a)) than in other parts.

4. Conclusion

Upon the investigation of the characteristics of friction surfaced using 5052 aluminum alloy plate and bar for the purpose of obtaining basic data on the friction surfaces, the following results were obtained.

(1) The circularly pattern due to the rotation of consumable rod was clearly observed on the surface of deposit, which became finer with increased rotational speed of consumable

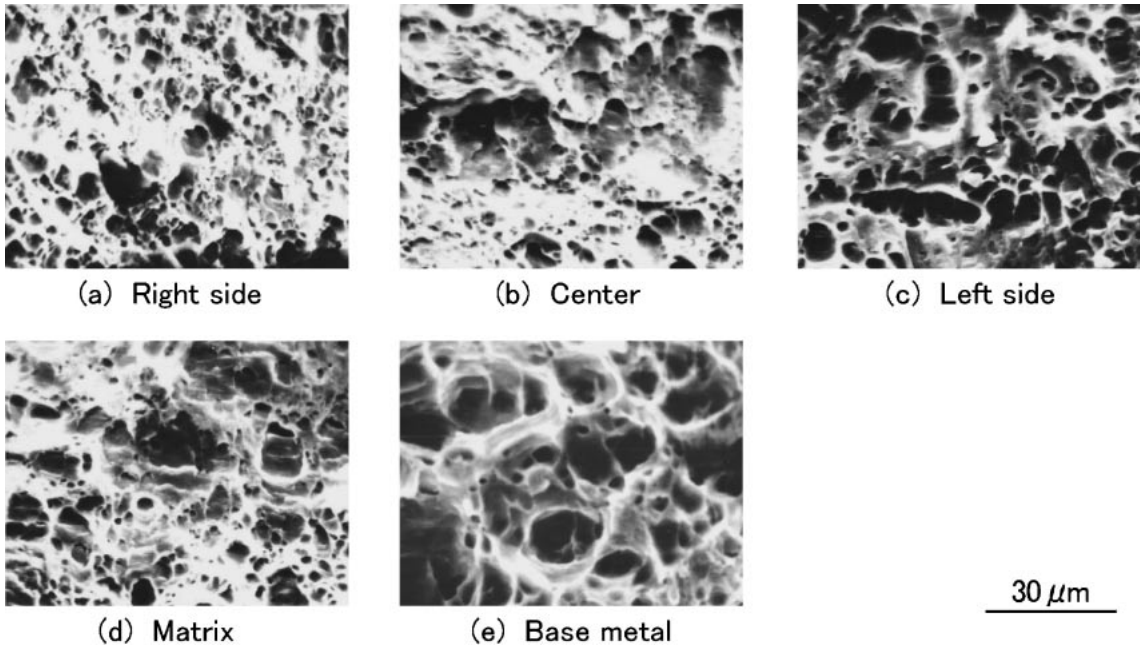

Fig. 13 Microfractographs of tensile tested specimens under conditions of friction pressure 40 MPa, rotational speed 33.3 s^{-1} and traverse speed 9 $mm \cdot s^{-1}$.

rod, with the width of deposit also becoming narrower. Also, the deposit tended to be clustered on the advancing side of deposit in the same direction as the consumable rod is shifted. This effect became greater with decreased rotational speed of consumable rod.

(2) The thickness of deposit became thinner with increasing rotational speed of consumable rod, and effect of traverse speed and friction pressure were decreased. The width of deposit was decreased with increased rotational speed and traverse speed of consumable rod, which was significant at low friction pressure.

(3) The surfacing efficiency, which was determined from the ratio of consumable rod weight before and after surfacing, decreased as a result of increased friction pressure and rotational speed of consumable rod, but increased with increased traverse speed.

(4) The macrostructure of the consumable rod enabled the weld interface between the deposit and substrate to be clearly identifiable at 20 MPa, the lowest friction pressure used in this experiment, but a small area of incomplete weld was observed at both sides of deposit. Defective weld was also observed. The defective weld disappeared after friction pressure was increased, with no defective weld observed at 40 MPa. The weld interface between deposit and substrate was difficult to identify at higher friction pressures.

(5) A fine structure was observed microscopically within the deposit, in contrast to the consumable rod and substrate. On the substrate, a fine structure, which appeared to be processed, was observed near the deposit. In peripheral areas, there was a slightly coarser structure, due to heat, than that of the substrate.

(6) Concerning temperature-time history during friction surfacing, the temperature started to increase immediately after the initiation of friction. The temperature gradient became steeper as the consumable rod, the heat source, came closer to the measurement point. The upper limit of the temperature range was lower by about 100-150 K than that seen in friction welding. The temperature on the advancing side of consumable rod was shifted was higher by about 52 K than that of the retreating side.

(7) There was a softening area, corresponding to the width of the deposit, at 1 mm as the nearest point from deposit. The width of softening area became narrower, and the hardness of softest point increased with increasing distance from deposit; the softening area disappeared at 3 mm from deposit.

(8) Tensile strength was slightly increased with increasing rotational speed and traverse speed of consumable rod, and tended to decrease slightly with increasing friction pressure. In this experiment, the highest tensile strength was 88.8% of that of the base metal of substrate. The extension under all conditions was higher than that of substrate.

Acknowledgements

A part of the research is supported by a grant from the Ministry of Education, Culture, Sport, Science, and Technology to Special Research grants for the development of characteristic education. Authors wish to express our sense of gratitude by making special mention here.

REFERENCES

1) T. Shinoda and Jinqi Li: J. Japan Inst. Light Metals **49** (1999) 499–503.
2) E. D. Nicholas and W. N. Thomas: Welding J. **65** (1986) 17–27.
3) Y. Kanbe, Y. Nakata, S. Kurihara, H. Koike and S. Miyake: Quarterly Journal of the Japan Welding Society **12** (1994) 82–88.
4) K. Fukakusa and T. Satoh: J. Japan Welding Society **50** (1981) 953–958.
5) A. Hasui and S. Fukushima: J. Japan Welding Society **44** (1975) 1005–1010.
6) K. Katoh and H. Tokisue: J. Japan Inst. Light Metals **49** (1999) 553–558.
7) K. Katoh and H. Tokisue: J. Light Metal Welding & Construction **32** (1994) 203–209.
8) K. Katoh and H. Tokisue: J. Japan Inst. Light Metals **36** (1986) 463–469.